AIR LOADS ON SOLAR PANELS DURING LAUNCH

W.M. Beltman, P.J.M. van der Hoogt, R.M.E.J. Spiering, H. Tijdeman

University of Twente, Faculty of Mechanical Engineering, P.O. Box 217,
7500 AE Enschede, The Netherlands, Tel. ++31-53-4892460, Fax ++31-53-4893695

ABSTRACT

The dynamical behaviour of solar panels during launch is significantly affected by the thin layers of air trapped between the panels. For narrow gaps the air manifests itself not only as a considerable added mass, but its viscosity can result in a substantial amount of damping. A model has been developed which describes the pressure distribution in the gap. The model includes the effects of inertia, viscosity, compressibility and thermal conductivity. The model is written in terms of dimensionless parameters which govern the motion of the air in the gap. For rigid panels, suspended in springs, located parallel to a fixed surface and performing translational or rotational oscillations, analytical solutions are presented. The results from specially designed experiments show good agreement with the analytical results. A large shift in eigenfrequency is observed and an increase in damping to almost critical values for narrow gaps. On the basis of the theory, a new acoustic finite element has been developed for the calculation of acousto-elastic interaction. Numerical results are shown for a flexible panel located parallel to a fixed surface.

1. INTRODUCTION

During launch solar panels are exposed to severe dynamic loads which might affect the satellite or its payload. For this reason it is essential to have accurate knowledge of the dynamical characteristics. The panels are folded against the body of the satellite (see figure 1). The thin layers of air, trapped between the panels, are of major importance for the dynamical behaviour of the system.

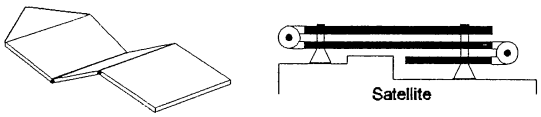

Fig. 1: Solar panels

The present paper deals with an important aspect that received very little attention in studies on the dynamical behaviour of solar panels: the viscous damping which is introduced by the thin layers of air trapped in the narrow gaps between the panels. In previous investigations the air was treated as inviscid [1]. For narrow gaps, however, the viscosity of the air can result in a significant amount of damping.

In the literature a number of investigations concern the effects of viscosity [2,3,4,5]. However, these investigations do not include the full acousto-elastic coupling between the vibrating rectangular panel and the thin layer of air. Especially for ligthweight structures a correct description of the coupling is inevitable. In this paper a new finite element model is described which enables fully coupled calculations for complex geometries, including the effects of viscosity and thermal conductivity.

2. THIN FILM THEORY

This chapter concerns the pressure distribution in the gap between a vibrating panel and a fixed surface. A rectangular panel with dimensions $2l_x$ x $2l_y$ is located parellel to a fixed surface and performs small oscillations (see figure 2). The distance between the panel and the surface is:

$$\bar{h}(\bar{x},\bar{y},t) = h_0\left[1 + h(\bar{x},\bar{y})\, e^{i\omega t}\right] \qquad (1)$$

In this expression h_0 is the mean gap width, h is the dimensionless amplitude of oscillation, i is the imaginary unit, ω is the angular frequency and t refers to time.

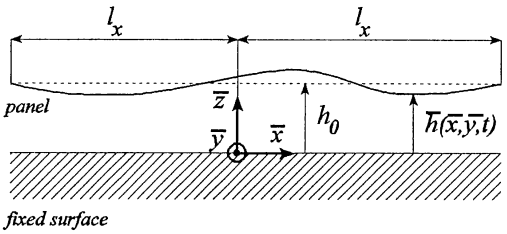

Fig. 2: Oscillating panel, located parallel to a fixed surface

Dimensionless co-ordinates are introduced according:

$$x = \frac{\bar{x}}{l_x} \quad ; \quad y = \frac{\bar{y}}{l_y} \quad ; \quad z = \frac{\bar{z}}{h_0} \qquad (2)$$

2.1 NARROW GAP EQUATION

The basic equations, governing the pressure distribution in the gap are the Navier Stokes equations, the equation of continuity, the equation of state for an ideal gas and the energy equation. The steady state conditions are: a zero mean velocity, a mean density ρ_0, a mean pressure p_0 and a mean temperature T_0. The velocities are written in a dimensionless form using the undisturbed speed of sound c_0. Following a similar approach as Tijdeman [6] small dimensionless perturbations (u, v, w, p, ρ, T) are introduced:

$$\begin{aligned} \bar{u} &= c_0\, u(x,y,z)\, e^{i\omega t} \quad ; \quad \bar{p} = p_0\left[1 + p(x,y,z)\, e^{i\omega t}\right] \\ \bar{v} &= c_0\, v(x,y,z)\, e^{i\omega t} \quad ; \quad \bar{\rho} = \rho_0\left[1 + \rho(x,y,z)\, e^{i\omega t}\right] \\ \bar{w} &= c_0\, w(x,y,z)\, e^{i\omega t} \quad ; \quad \bar{T} = T_0\left[1 + T(x,y,z)\, e^{i\omega t}\right] \end{aligned} \qquad (3)$$

When higher order terms are neglected, the basic equations can be written in a linear, non-dimensional form. In the equations six dimensionless parameters can be distinguished :

Proc. Conference on Spacecraft Structures, Materials & Mechanical Testing, Grand Hotel Huis ter Duin, Noordwijk, The Netherlands, 27–29 March 1996 (ESA SP-386, June 1996)

$$s = h_0\sqrt{\frac{\rho_0\,\omega}{\mu}} \quad : \textit{shear wave number}$$

$$\sigma = \sqrt{\frac{\mu\,C_p}{\lambda}} \quad : \textit{square root of Prandtl number}$$

$$k = \frac{\omega\,h_0}{c_0} \quad : \textit{reduced frequency} \qquad (4)$$

$$\gamma = \frac{C_p}{C_v} \quad : \textit{ratio of specific heats}$$

$$g = \frac{h_0}{l_x} \quad : \textit{narrowness of the gap}$$

$$a = \frac{l_y}{l_x} \quad : \textit{aspect ratio of panel}$$

In these expressions μ denotes the viscosity, λ the thermal conductivity, C_p the specific heat at constant pressure and C_v the specific heat at constant volume. The most important parameter is the shear wave number, s, which is a measure for the ratio between the inertial forces and the viscous forces. The reduced frequency k is a measure for the ratio between the gap width and the acoustic wave length. When the gap width is small in comparison with the acoustic wave length, i.e. $k \ll 1$, and the in-plane velocities are large compared to the velocity in the z-direction, the aforementioned basic equations can be simplified to:

$$i\,u = -\frac{g}{k}\frac{1}{\gamma}\frac{\partial p}{\partial x} + \frac{1}{s^2}\frac{\partial^2 u}{\partial z^2} \qquad (a)$$

$$i\,v = -\frac{g}{a\,k}\frac{1}{\gamma}\frac{\partial p}{\partial y} + \frac{1}{s^2}\frac{\partial^2 v}{\partial z^2} \qquad (b)$$

$$0 = -\frac{1}{k}\frac{1}{\gamma}\frac{\partial p}{\partial z} \qquad (c) \qquad (5)$$

$$-i\,k\,\rho = \frac{\partial u}{\partial x} + \frac{g}{a}\frac{\partial v}{\partial y} + \frac{\partial w}{\partial z} \qquad (d)$$

$$p = \rho + T \qquad (e)$$

$$i\,T = \frac{1}{s^2\sigma^2}\frac{\partial^2 T}{\partial z^2} + i\left[\frac{\gamma - 1}{\gamma}\right]p \qquad (f)$$

The z-component of the Navier Stokes equations, i.e. (5a), learns that the pressure is constant across the gap width. The energy equation, i.e. (5f), can now be solved. The following boundary conditions apply:

$$z = 0: \quad u = 0 \;;\; v = 0 \;;\; T = 0 \;(\textit{isothermal wall}) \qquad (6)$$
$$z = 1: \quad u = 0 \;;\; v = 0 \;;\; T = 0 \;(\textit{isothermal wall})$$

With these boundary conditions, the equations (5) can be rewritten into one equation in terms of the pressure perturbation, the so-called *narrow gap equation* [7]:

$$g^2\frac{\partial^2 p}{\partial x^2} + \frac{g^2}{a^2}\frac{\partial^2 p}{\partial y^2} + \frac{k^2\gamma}{n\,B(s)}p = -\frac{k^2\gamma}{B(s)}h(x,y) \qquad (7)$$

where:

$$B(s) = 2\left[\frac{1-\cosh(s\sqrt{i})}{s\sqrt{i}\,\sinh(s\sqrt{i})}\right] + 1 \qquad (8)$$

$$n = \left[1 - \left[\frac{\gamma - 1}{\gamma}\right]B(s\sigma)\right]^{-1} \qquad (9)$$

The energy equation and the equation of state can be replaced by the polytropic relation:

$$\frac{\bar{p}}{\bar{\rho}^n} = \textit{constant} \qquad (10)$$

with n being the polytropic constant as given in expression (9). This complex polytropic constant accounts for the effects of thermal conductivity. Note that the product $s\sigma$ is not affected by the value of the viscosity μ (see (4)).

2.2 THE SHEAR WAVE NUMBER

As mentioned before, the shear wave number represents the ratio between inertial forces and viscous forces. For high shear wave numbers ($s \gg 1$) the viscous effects are negligible, whereas for low shear wave numbers ($s \ll 1$) the inertial effects can be neglected. The shear wave number can be interpreted as the ratio between the gap width and the boundary layer thickness. The importance of the shear wave number can be illustrated with the velocity profile in the gap. The shape of the magnitude of the in-plane velocity, u, is depicted in figure 3 for shear wave numbers of 0.5, 10 and 100.

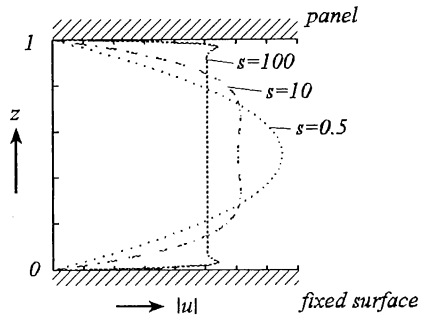

Fig. 3: Velocity profile in the gap for various shear wave numbers

For low shear wave numbers a parabolic velocity profile is obtained, whereas for high shear wave numbers the velocity profile is flat. Figure 3 clearly shows the transition from inertial dominated flow to viscosity dominated flow. The dimensionless parameters are very useful for a quick estimation of the importance of viscous and thermal effects.

2.3 LOW SHEAR WAVE NUMBERS: REYNOLDS EQUATION

For low shear wave numbers the inertial forces can be neglected compared to the viscous forces. The function $B(s)$ can be approximated by:

$$B(s) = \frac{1}{12} i s^2 \qquad (11)$$

The value for the polytropic constant n in (9) now reduces to 1. This implies that the process can be regarded as isothermal. When these relations are substituted in the narrow gap equation, a linearized version of the well known Reynolds equation is obtained.

2.4 HIGH SHEAR WAVE NUMBERS: WAVE EQUATION

For high shear wave numbers the viscous forces can be neglected compared to the inertial forces. The function $B(s)$ can be approximated by:

$$B(s) = 1 \qquad (12)$$

The polytropic constant n now reduces to γ: the process is adiabatic (isentropic). For this situation, a modified form of the wave equation is obtained. The modification is due to the assumption that the pressure is constant across the gap width.

2.5 EFFECTIVE SPEED OF SOUND

The narrow gap equation (7) can be rewritten in the following form:

$$\frac{\partial^2 \bar{p}}{\partial \bar{x}^2} + \frac{\partial^2 \bar{p}}{\partial \bar{y}^2} + \frac{\omega^2 \gamma}{c_0^2 n B(s)} \bar{p} = -\frac{\rho_0 \omega^2}{B(s)} h \qquad (13)$$

A comparison with the classical wave equation learns that the standard acoustic wave number (ω/c_0) is replaced by a complex quantity. Equation (13) indicates that the effects of viscosity and thermal conductivity can be interpreted in terms of an effective speed of sound:

$$c_{eff}(s) = c_0 \sqrt{\frac{n}{\gamma} B(s)} \qquad (14)$$

The effective speed of sound is affected by thermal effects, accounted for in the polytropic constant n, and viscous effects, accounted for in the function $B(s)$.

3. OSCILLATING RIGID PANELS

Calculations and experiments were carried out with oscillating, rigid solar panels in order to verify the model.

3.1 TRANSLATING PANEL

A rectangular solar panel is suspended in springs at the corners. The panel is located parallel to a fixed surface and performs a small, normal oscillation. The mean distance between the panel and the fixed surface, h_0, can be varied.

Calculations

The amplitude of oscillation is constant for all points on the panel, i.e. the dimensionless amplitude h is not a function of x or y.

$$\bar{h}(x,y,t) = h_0 \left[1 + h e^{i\omega t}\right] \qquad (15)$$

The narrow gap equation for this case yields:

$$g^2 \frac{\partial^2 p}{\partial x^2} + \frac{g^2}{a^2} \frac{\partial^2 p}{\partial y^2} + \frac{k^2 \gamma}{n B(s)} p = -\frac{k^2 \gamma}{B(s)} h \qquad (16)$$

The boundary conditions for this equation are (open ends):

$$\begin{aligned} x = -1 &: p = 0 \quad ; \quad x = 1 : p = 0 \\ y = -1 &: p = 0 \quad ; \quad y = 1 : p = 0 \end{aligned} \qquad (17)$$

The solution for (16), with boundary conditions (17), is:

$$p(x,y) = -\frac{4 k^2 \gamma h a^2}{\pi g^3 B(s)} \sum_{q=1,3,..} \frac{(-1)^{\frac{q-1}{2}}}{q D^2} \left[1 - \frac{\cosh(Dy)}{\cosh(D)}\right] \cos\left[\frac{q\pi}{2} x\right] \qquad (18)$$

where:

$$D = \sqrt{\left[\frac{q\pi}{2} a\right]^2 - \frac{k^2 a^2 \gamma}{g^2 n B(s)}} \qquad (19)$$

The pressure distribution can be integrated over the surface in order to obtain the dimensionless air load, acting on the panel:

$$\frac{\bar{F}}{p_0 l_x l_y} = \int\int p \, dx \, dy = \frac{32 k^2 \gamma h a^2}{\pi^2 g^3 B(s)} \sum_{q=1,3,..} \frac{1}{q^2 D^2} \left[1 - \frac{\tanh(D)}{D}\right] \qquad (20)$$

The air load affects the dynamical behaviour of the system. Once the air load is determined, the eigenfrequency and the corresponding damping coefficient can be calculated. The influence of the air on the upper side of the panel is not taken into account. For narrow gaps the influence of the air on the upper side of the panel can be neglected compared to the influence of the air in the gap. Since this investigation deals with narrow gaps and the film theory is only valid for narrow gaps, this assumption is justified.

Experiments

The experiments were carried out with a solar panel of 0.98 x 0.98 m with a mass of only 2.5 kg. The panel was suspended in 8 springs, 2 located at the top and bottom of each corner.

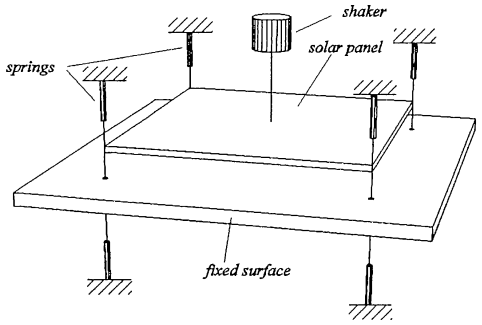

Fig. 4: Experimental setup translating panel

The eigenfrequency of the panel-spring system in vacuum is calculated to be 9.74 Hz. Due to the influence of the air, the eigenfrequency will decrease. The frequency range of interest therefore was 1 to 10 Hz. This is far below the first elastic eigenfrequency of the panel. Accelerometers were mounted on the panel in order to verify the assumption of rigid behaviour. In the mentioned frequency range the deformation of the panel was negligible. The panel was excited with an electrodynamic shaker. The fixed surface was a rectangular rigid plate of 2.2 x 1.8 m, which was mounted on a frame parallel to the panel. The distance between the plate and the fixed surface was varied between 3 and 50 mm. The shear wave number for this configuration varied between 1.9 and 100. This implies that for narrow gaps the viscous forces are of the same order of magnitude as the inertial forces. The properties of the air under standard atmospheric conditions and the panel are:

$$\begin{aligned} &Air: && \mu\text{-}18.2\ 10^{-6}\ Ns/m^2 \\ &\lambda\text{-}25.6\ 10^{-3}\ W/mK\ ;\ \rho_0\text{-}1.2\ kg/m^3\ ;\ c_0\text{-}340\ m/s && (21) \\ &C_p\text{-}1004\ J/kgK\ ;\ C_v\text{-}716\ J/kgK\ ;\ T_0\text{-}290\ K \end{aligned}$$

$$\begin{aligned} &Panel: && m\text{-}2.516\ kg\ ;\ \kappa\text{-}1178\ N/m \\ &&& l_x\text{-}0.49\ m\ ;\ l_y\text{-}0.49\ m \end{aligned} \qquad (22)$$

where m denotes the mass of the panel and κ is the stiffness of one spring. The measured eigenfrequency (phase resonance), f_n, and the damping coefficient, ξ, are listed in table I [8].

Results

The experimental results and the analytical results are depicted in the figures 5 and 6. These figures learn that the eigenfrequency shows a strong decrease with decreasing gap width, whereas the damping shows a strong increase. For a gap of 3 mm the damping is almost critical. Calculations and experiments show fair agreement.

h_0 (mm)	f_n (Hz)	ξ (%)	h_0 (mm)	f_n (Hz)	ξ (%)
50	7.574	0.29	8	4.977	5.03
35	7.254	0.53	6	4.511	8.04
25	6.801	0.94	4	3.809	18.6
15	6.035	1.80	3	3.223	44.1
10	5.402	3.52			

Table I: Experimental results translating panel [8]

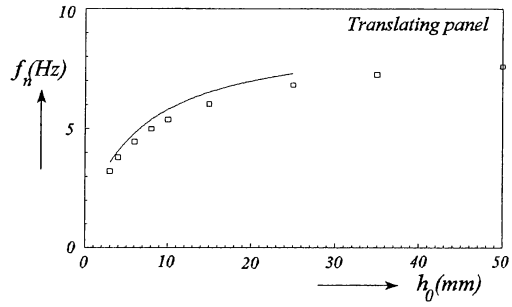

Fig. 5: Eigenfrequency f_n as function of gap widt h_0
_____ : analytical ; □ : measurements

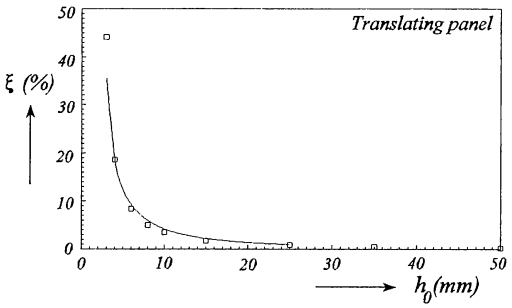

Fig. 6: Damping coefficient ξ as function of gap width h_0
_____ : analytical ; □ : measurements

For narrow gaps there is a strong pumping effect: the air has to move back and forth in the gap. This pumping effect results in a considerable added mass and a substantial damping for the panel. For the panel under consideration, the added mass for a gap of 3 mm is 20 kg, while the mass of the panel itself is only 2.5 kg. The added mass can be extracted from the shift in eigenfrequency. Because of the high damping values involved, it is important to distinguish between the amplitude resonance frequency and the phase resonance frequency. The amplitude resonance frequency, i.e. the frequency corresponding to a maximum peak value in the transfer function between force and displacement, is affected by the amount of viscous damping. When this frequency would be used to calculate the amount of added mass, a shift in frequency due to damping is wrongly attributed to added mass. The phase resonance frequency is not affected by the damping.

3.2 PANEL ROTATING AROUND CENTRAL AXIS

Again, a solar panel is located parallel to a fixed surface. This time it performs a small, angular oscillation around an axis of rotation which is located in the mid of the panel ($x=0$). The mean distance between the panel and the fixed surface h_0 can be varied.

Calculations

The distance between panel and surface for the small angular rotation around $x=0$ can be written as:

$$\bar{h}(x,y,t) = h_0\left[1 + \frac{\alpha}{g} x\, e^{i\omega t}\right] \qquad (23)$$

where α is the amplitude of the angular oscillation. The narrow gap equation for this case reads:

$$g^2\frac{\partial^2 p}{\partial x^2} + \frac{g^2}{a^2}\frac{\partial^2 p}{\partial y^2} + \frac{k^2\gamma}{nB(s)}p = -\frac{k^2\gamma\alpha}{gB(s)}x \qquad (24)$$

The boundary conditions for this equation are (open ends):

$$\begin{aligned} x = -1:\ p = 0 \quad ; \quad x = 1:\ p = 0 \\ y = -1:\ p = 0 \quad ; \quad y = 1:\ p = 0 \end{aligned} \qquad (25)$$

Equation (24), with boundary conditions (25), can be solved:

$$p(x,y) = -\frac{4k^2\gamma\alpha a^2}{\pi g^3 B(s)} \sum_{q=2,4,..} \frac{1}{q}\frac{(-1)^{\frac{q-1}{2}}}{D^2}\left[1 - \frac{\cosh(Dy)}{\cosh(D)}\right]\sin\left[\frac{q\pi}{2}x\right] \qquad (26)$$

where:

$$D = \sqrt{\left[\frac{q\pi}{2}a\right]^2 - \frac{k^2a^2\gamma}{g^2 nB(s)}} \qquad (27)$$

Because the pressure distribution is asymmetric with respect to x, the net normal force on the panel is zero. For an angular oscillation the dimensionless aerodynamic moment acting on the panel can be calculated:

$$\frac{\bar{M}}{p_0 l_x^2 l_y} = \int\int xp\, dx\, dy = -\frac{32k^2\gamma\alpha a^2}{\pi^2 g^3 B(s)} \sum_{q=2,4,..} \frac{1}{q^2 D^2}\left[1 - \frac{\tanh(D)}{D}\right] \qquad (28)$$

Once the aerodynamic moment is determined, the eigenfrequency of the system and the corresponding damping coefficient can be calculated. Again, the influence of the air on the upper side of the panel is not taken into account. For narrow gaps the influence of the air on the upper side can be neglected compared to the influence of the air in the gap.

Experiments

The experiments were carried out with a solar panel of 1.67 x 1.29 m. The mass moment of inertia of the panel was 1.53 kgm^2. The panel was suspended in 8 springs, 2 located in each of the four points on the side edges of the panel (see figure 7).

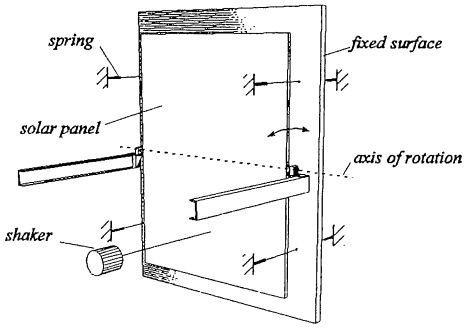

Fig. 7: Experimental setup rotating panel

The eigenfrequency of the panel-spring system in vacuum was 2.96 Hz. Due to the influence of the air, the eigenfrequency will decrease. The frequency range of interest therefore is 1 to 3 Hz. Accelerometers were mounted on the plate in order to verify the rigidness of the panel. In the mentioned frequency range the deformation of the panel was negligible. The panel was excited with an electrodynamic shaker. The fixed surface was a rectangular rigid plate of 2.2 x 1.8 m, which was mounted on a frame parallel to the panel. The distance between the plate and the fixed surface was varied between 3 and 50 mm. The shear wave number for this configuration varies between 1.9 and 55. This implies that for narrow gaps the viscous forces are of the same order of magnitude as the inertial forces. The properties of the air were taken identical to (21). The remaining properties of interest are:

$$\begin{aligned} I = 1.53\ kg\,m^2 \ ; \ \kappa = 1959\ N/m \\ l_x = 0.835\ m \ ; \ l_y = 0.645\ m \ ; \ l_{spr} = 0.644\ m \end{aligned} \qquad (29)$$

where I denotes the mass moment of inertia of the panel, κ is the stiffness of one spring and l_{spr} denotes the distance between the springs and the axis of rotation. The measured eigenfrequency (phase resonance), f_n, and damping coefficient, ξ, are listed in table II [9].

h_0 (mm)	f_n (Hz)	ξ (%)	h_0 (mm)	f_n (Hz)	ξ (%)
50	2.560	0.52	10	1.967	5.10
35	2.471	0.77	8	1.851	7.60
25	2.363	1.20	6	1.712	13.0
20	2.280	1.70	4	1.506	31.0
15	2.164	2.60	3	1.421	49.0

Table II: Experimental results rotating panel [9]

Results

The experimental results and the analytical results are depicted in the figures 8 and 9. Figure 8 learns that the eigenfrequency of the system decreases with decreasing gap width. The damping shows a strong increase to almost critical with decreasing gap width. Calculations and experiments show fair agreement.

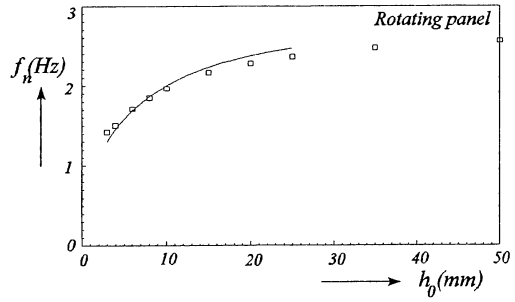

Fig. 8: Eigenfrequency f_n as function of gap width h_0
_____ : analytical ; □ : measurements

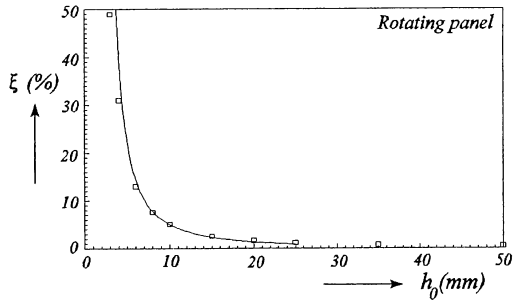

Fig. 9: Damping coefficient ξ as function of gap width h_0
_____ : analytical ; □ : measurements

For the rotating panel, the shift in eigenfrequency can be interpreted as an added mass moment of inertia. The mass moment of inertia of the panel itself is 1.5 kg m^2. For a gap of 3 mm the added mass moment of inertia due to the air is 5.5 kg m^2.

3.3 PANEL ROTATING AROUND ARBITRARY AXIS

Consider a rigid panel, located parallel to a fixed surface and performing a small, angular oscillation with amplitude α around for instance the axis $x=x_{axis}$. The distance between panel and fixed surface for this situation is:

$$\bar{h}(x,y,t) = h_0\left[1 + \frac{\alpha}{g}(x - x_{axis})e^{i\omega t}\right] \qquad (30)$$

The narrow gap equation for this case is:

$$g^2\frac{\partial^2 p}{\partial x^2} + \frac{g^2}{a^2}\frac{\partial^2 p}{\partial y^2} + \frac{k^2\gamma}{nB(s)}p = -\frac{k^2\gamma\alpha}{gB(s)}[x - x_{axis}] \qquad (31)$$

This equation learns that the pressure distribution is composed of two parts: the pressure distribution for a translating panel with amplitude $h = -\alpha x_{axis}/g$ and the pressure distribution for a panel rotating around $x=0$ with amplitude α. The position of the axis of rotation determines the ratio between the translational and the rotational contribution. Evidently, the pressure distribution can be calculated by simply taking the appropriate linear combination of the solutions from the sections 3.1 and 3.2. A similar relation holds for a rotation around an axis $y=y_{axis}$. With these solutions a rigid motion around an arbitrary axis can be described.

4. ACOUSTO-ELASTIC COUPLING: FINITE ELEMENT FORMULATION

The theory, as decribed in section 2, can be used to calculate the interaction between a flexible structure and a viscous layer of gas or fluid. Analytical solutions for this type of interaction problems can only be found for simple configurations. In order to be able to model the interaction for more complex geometries, a finite element model was developed.

4.1 STRUCTURAL MODEL

The dynamical behaviour of the structure is modelled with standard plate or solid elements. In the absence of damping the finite element formulation for harmonic vibrations can be written as:

$$-\omega^2[M_s]\{U\} + [K_s]\{U\} = \{F_s\} \qquad (32)$$

where $[M_s]$ is the mass matrix, $[K_s]$ is the stiffness matrix, $\{U\}$ is the vector with the nodal displacement degrees of freedom and $\{F_s\}$ is the external nodal force vector.

4.2 ACOUSTIC MODEL

The pressure distribution in the air is governed by the narrow gap equation (see section 2). The dimensionless equation can be rewritten to (13,14):

$$\frac{\partial^2\bar{p}}{\partial\bar{x}^2} + \frac{\partial^2\bar{p}}{\partial\bar{y}^2} + \frac{\omega^2}{c_{eff}^2(s)}\bar{p} = -\frac{\rho_0\omega^2}{h_0 B(s)}h_0 h(x,y) \qquad (33)$$

This equation is used to set up the finite element formulation for the pressure distribution in the gap. This finally gives:

$$-\omega^2[M_a(s)]\{P\} + [K_a]\{P\} = \{F_a\} \qquad (34)$$

where $[M_a]$ is the acoustic mass matrix, $[K_a]$ is the acoustic stiffness matrix, {P} is the vector with the nodal pressure degrees of freedom and $\{F_a\}$ is the external nodal force vector. An acoustic viscous finite element has been implemented in the finite element code B2000 [10].

It has to noted that the acoustic mass matrix is a complex and frequency dependent matrix. The new element contains a number of key options which can be used to rule out viscous or thermal effects. This enables a comparison with, for instance, inviscid behaviour of the air.

4.3 ACOUSTO-ELASTIC MODEL

The coupling between a vibrating flexible structure and the layer of gas is established by demanding continuity of velocity across the interface. With this interface condition, the finite element models for structure and gas layer are coupled:

$$-\omega^2\begin{bmatrix}[M_s] & [0]\\ [M_c] & [M_a(s)]\end{bmatrix}\begin{Bmatrix}\{U\}\\ \{P\}\end{Bmatrix}+\begin{bmatrix}[K_s] & [-K_c]\\ [0] & [K_a]\end{bmatrix}\begin{Bmatrix}\{U\}\\ \{P\}\end{Bmatrix}=\begin{Bmatrix}\{F_s^{ext}\}\\ \{0\}\end{Bmatrix} \quad (35)$$

where the coupling matrces $[M_c]$ and $[K_c]$ are related by:

$$[M_c]=\frac{\rho_0 c_0^2}{h_0 B(s)}[K_c]^T \quad (36)$$

The resulting set of equations is complex and asymmetric.

4.4 EXAMPLE: FLEXIBLE SOLAR PANEL

As an example, the interaction between a flexible solar panel and a thin layer of air was calculated. The example was taken from Grooteman & Schippers [1], who performed similar calculations. Their approach, however, was based on the wave equation: no viscous or thermal effects.

Setup

A rectangular solar panel of 1.675 x 1.25 m is located parallel to a fixed surface. The panel is simply supported along the short sides and free along the long sides (see figure 10).

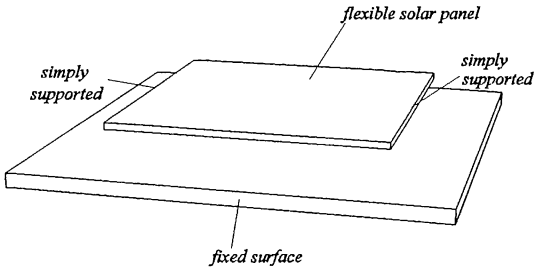

Fig. 10: Flexible solar panel, located parallel to a fixed surface; short sides simply supported, long sides free

The air between the panel and the fixed surface is free to flow in and out of the gap: open ends. The properties of the air are taken according to (21). The properties of the panel are equivalent properties: the honeycomb structure of the solar panel is replaced by a homogeneous panel with corresponding equivalent properties.

The equivalent properties of the panel are:

$$\rho_s = 1122.2\ kg/m^3\ ;\ l_x = 0.8375\ m\ ;\ l_y = 0.625\ m$$
$$E_s = 4.5444\ 10^{13}\ N/m^2\ ;\ \nu_s = 0.3\ ;\ t_s = 1\ mm \quad (37)$$

where ρ_s is the density of the panel, E_s is Young's modulus, ν_s is Poisson's ratio and t_s is the thickness of the panel.

Calculations

The panel is modelled with 16 x 16 four noded shell elements. The air in the gap is modelled with 16 x 16 four noded viscous acoustic elements. Interface elements are used to establish the coupling between the plate and the acoustic elements. The influence of the air on the upper side of the panel is not taken into account, because its influence can be neglected for narrow gaps. On the boundaries of the acoustic domain the pressure disturbance is set to zero.

Results

The eigenfrequencies of the panel in vacuum are calculated and compared to approximate frequencies taken from the Blevins [11]. The results are listed in Table III.

mode	Blevins (Hz)	B2000 (Hz)
1	34.09	33.25
2	68.67	68.58
3	136.4	136.7
4	181.1	182.3

Table III: Eigenfrequencies of the panel in vacuum

The table learns that the number of elements is large enough to give accurate results for the lower modes.

The first eigenfrequency and the corresponding damping coefficient for the flexible panel were calculated as a function of gap width. Two types of calculations were carried out. One calculation included the effects of viscosity and thermal conductivity. The second calculation was based on a modified wave equation: $B(s)$ was set to 1 and n was set to γ (see section 2.4). The first eigenfrequency of the panel f_1 as a function of the gap width is depicted in figure 11. The corresponding damping coefficient ξ is depicted in figure 12.

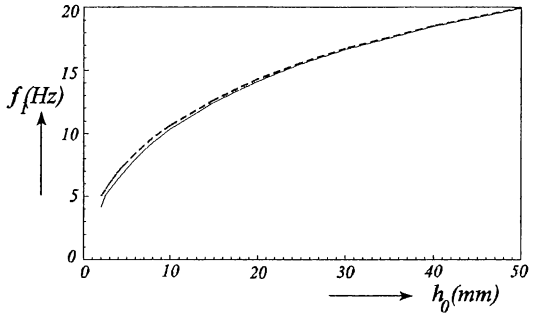

Fig. 11: Eigenfrequency f_1 as function of gap width h_0
_____ : viscous ; __ __ : inviscid

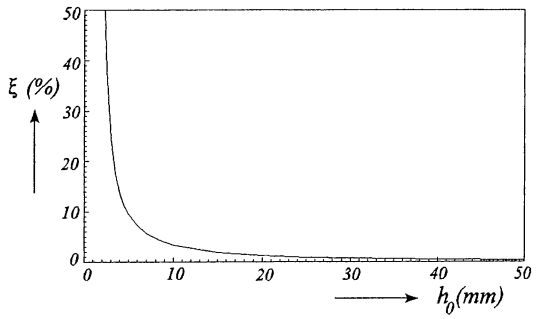

Fig. 12: Damping coefficient ξ as function of gap width h_0
_____ : viscous ; (inviscid calculation gives zero damping)

Physical interpretation

The shift in eigenfrequency can be used to extract the amount of generalized added mass for the panel. For a gap of 10 mm the generalized added mass is 22 kg, while for a gap of 3 mm the added mass is 82 kg. This example illustrates the large shift in frequency due to the added mass effect. Another interesting observation can be made in figure 11 by comparing the values from the viscous and the inviscid calculations. The figure shows that the viscosity and the thermal conductivity of the air result in a small extra added mass. At first sight this seems strange, since one would expect the viscosity to affect the damping, but not the added mass. However, due to the effects of viscosity the velocity profile in the gap changes (see section 2.2 and figure 3). This change in velocity profile causes the change in added mass.

For narrow gaps the air not only manifests itself as an added mass, but also as a considerable damping (see figure 12). Evidently, for low values of the shear wave number viscosity and heat conduction have to be taken into account. The shear wave number, evaluated at the eigenfrequency, is depicted in figure 13.

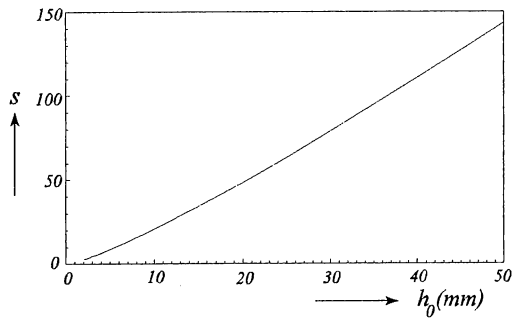

Fig. 13: Shear wave number as function of gap width h_0

The figure learns that for the present configuration with narrow gaps the effects of viscosity cannot be discarded.

5. CONCLUSIONS

A model is presented which describes the pressure distribution in a thin layer of air between vibrating surfaces. The motion of the air is governed by a number of dimensionless parameters. The most important parameter is the shear wave number: the ratio between inertial forces and viscous forces. The model has been validated for oscillating, rigid panels. Analytical results and experimental results show good agreement. Based on this model, a new finite element was implemented in the program B2000. This enables fully coupled acousto-elastic calculations for complex geometries, including the effects of viscosity and thermal conductivity. Calculations illustrate the significant influence of viscosity and heat conduction for low shear wave numbers.

6. ACKNOWLEDGEMENTS

The experiments were carried out by E.G. van de Veen and H.J. Brink. The measurements were supervised by A.G.M. Wolbert. The support from J.J. Wijker (Fokker Space), who supplied the solar panels, is gratefully acknowledged.

7. REFERENCES

1 Grooteman FP & Schippers H, 1994, Coupled analysis in acoustics on the dynamical behaviour of solar arrays, *Proc. ISMA19 Tools for Noise and Vibration Analysis*, Sas P (ed), Leuven, 125-137

2 Önsay T, 1993, Effects of layer thickness on the vibration response of a plate-fluid layer system, *Journal of Sound and Vibration*, 163(2), 231-259

3 Önsay T, 1994, Dynamic interactions between the bending vibrations of a plate and a fluid layer attenuator, *Journal of Sound and Vibration*, 178(3), 289-313

4 Fox MJH & Whitton PN, 1980, The damping of structural vibrations by thin gas films, *Journal of Sound and Vibration*, 73(2), 279-295

5 Trochidis A, 1982, Körperschalldämpfung mittels Gas oder Flüssigkeitsschichten, *Acustica*, 51(4), 201-212

6 Tijdeman H, 1975, On the propagation of sound in cylindrical tubes, *Journal of Sound and Vibration*, 39(1), 1-33

7 Beltman WM, 1994, Forces on a rigid plate oscillating normal to a fixed surface, University of Twente, Faculty of Mechanical Engineering, report WB.94/TM-943

8 Veen EG van de, 1994, Onderzoek aan een harmonisch translerende starre plaat in lucht, University of Twente, Faculty of Mechanical Engineering, report WB.94/TM-945 (in Dutch)

9 Brink HJ, 1995, Luchtkrachten op een paneel dat een oscillerende rotatiebeweging uitvoert, University of Twente, Faculty of Mechanical Engineering, Graduation report (in Dutch)

10 Merazzi S, 1994, Modular finite element analysis tools applied to problems in engineering, PhD thesis 1251, EPFL Lausanne, Switserland

11 Blevins RD, 1979, Formulas for natural frequency and mode shape, Van Nostrand Reinholds company, New York